to be homogeneous. This approach can be used to discriminate a large number of object classes by properly choosing the texton, but can yield wrong results if the texton parameters are selected inappropriately. In contrast, we focus on the discrimination of only two object classes (grassland and cropland).

Additional methods for the determination of structural features are the Fourier and Radon transformation. Chanussot et al. (2005) estimate the orientation of vineyard rows automatically using the Fourier spectrum of a pre-processed image and its Radon transformation. However, the authors apply their method to high resolution aerial data only, and furthermore, a very important assumption is a regular spacing between the rows. This assumption is usually satisfied for vineyards, but not necessarily for cropland. In cropland the distance between rows can vary from one field to the next, depending on the culture of vegetation, and the kind of machine which was used, and furthermore, the visibility of the structures in the image of one field.

A huge number of publications deals with various approaches of orientation estimation.. Le Pouliquen et al. (2002) use convolution masks for a scale-adaptive orientation estimation which is divided into a gradient based and valleyness operator. Compared to this approach, De Costa et al. (2002) use orientation difference histograms. The focus of the approach of De Costa et al. is not the quantitative estimation of the direction, instead only the existence of a direction is of interest. This idea is also sufficient to characterize cropland. However, both approaches were tested for synthetic images only.

Warner and Steinmaus (2005) identify orchards and vineyards in IKONOS panchromatic imagery. In this approach the classes are detected using autocorrelation. After the definition of a square kernel and the normalization of each pixel of this kernel the autocorrelation for the cardinal directions and both diagonals is determined. For each autocorrelation calculation (called autocorrelogram) each pixel is analyzed separately to identify orchards. An orchard pixel is detected if an orchard pattern is identified in more than one autocorrelogram centered on the same pixel. However, the trees have to be approximately equally spaced. Similar to the aforementioned approach of Chanussot et al. (2005) this assumption is usually not met in cropland.

Radiometric features were used by Itzerott and Kaden (2006 and 2007) to discriminate between various farmland types. They analysed typical economic plants and grassland in the German federal state of Brandenburg. It was shown that grassland possesses a non-zero NDVI (**N**ormalised **D**ifference **V**egetation **I**ndex) in all seasons, whereas during the winter season several agricultural plants have a very low NDVI which is significantly different from the NDVI of grassland.

The literature review shows that some work on the classification of farmland types using structural and radiometric features has been done. However, either the approaches rely on training samples or on precise knowledge on the structure or radiometric properties of the field class, i.e. they are model-driven. For our approach we want to be independent of such conditions and therefore persue a more data-driven approach.

3. AUTOMATIC DISCRIMINATION OF FARMLAND TYPES

3.1 Workflow of WiPKA-QS

The aim of the project WiPKA-QS is the automated verification of the German topographic reference dataset ATKIS*** or in general GIS. The main components of ATKIS are the object based digital landscape models (DLM) encompassing several resolutions with a geometric accuracy of up to +/-3m.

The core of the automated procedure is the knowledge-based image interpretation system GeoAIDA (Bückner et al., 2002). GeoAIDA uses a semantic network that represents the scene to be analyzed. First, in a top-down or so called model-driven step, the system searches for evidence for the object to be verified in the orthoimage. Evidence can be the existence of a main direction of cultivation. Thereby, the system focuses only on objects of interest. Afterwards, in the bottom-up or so called data-driven step, the system derives an acceptance or rejection decision assessing the evidence. Hence, discrepancies between objects and the image features can be detected. Is the verification of an object successful the system labels this object as accepted (green); otherwise the object is labelled as rejected (red). For the rejected objects, a final decision is made by a human operator. Further details of the system are available in (Busch et al, 2004) and furthermore in (Müller and Zaum, 2005), its workflow is sketched in Figure 1.

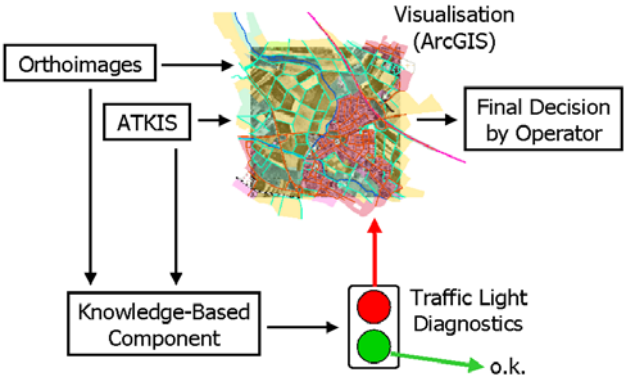

Figure 1: Workflow WiPKA-QS

3.2 Strategy

The underlying semantic model of the approach is shown in Figure 2. The first level of the semantic net describes the *Real World*: farmland can contain cropland and grassland, and furthermore cropland consists of untilled or tilled cropland. The second level *Geometry/Material* explains the geometrical and material characteristic of the objects. Finally, the *Imagery* level shows the characteristics which are visible in the image.

*** **A**mtlich **t**opographisch-**k**artographisches **I**nformationssystem (Authoritative Topographic Cartographic Information System)

Thus, parallel lines are mapped into points situated vertically above each other, assuming the ϕ-parameter is mapped to the horizontal axis in Hough space. Furthermore, if the space between lines in image space is constant, a periodicity of the point positions in Hough space is observable.

By extracting these points in the Hough image we focus on salient lines in image space. Points are extracted using the Förstner operator (Förstner and Gülch, 1987) and are called points of interest (POI).

3.3.3 Orientation Estimation

In the next step, a histogram of the extracted points along the ϕ–axis in Hough space is derived. The histogram of the previous cropland object is shown in Figure 6. The unit for ϕ on the x-axis is grad, the y-axis shows the number of occurrences of the angles.

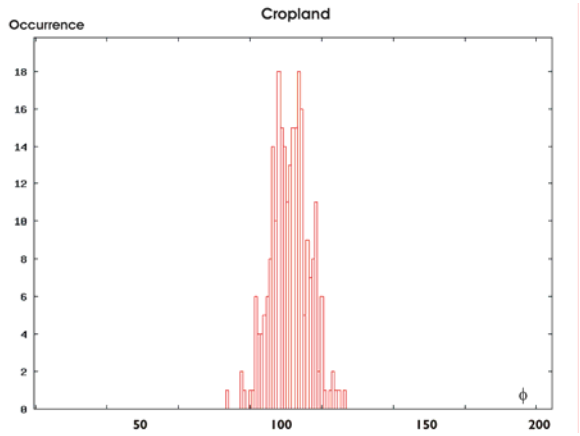

Figure 6: Histogram of angles in Hough Space of Figure 5 (right)

3.3.4 Assessment

As a final step we investigate the in the histogram probable direction of cultivation by computing the largest peak in the histogram, and in addition the standard deviation σ for this peak. For cropland σ must lie below a pre-defined threshold t, whereas for grassland σ is assumed to le larger than t. In addition, a number of at least s lines with the same direction must have been detected. The parameters s and t are defined heuristically. In Figure 6 σ amounts to approximately 5grad and at least 5 lines with the same direction are detectable. Finally, the object depicted in Figure 4 is accepted as a cropland object.

3.4 Examples and Evaluation

The described approach was implemented and tested on a number of IKONOS images. Here, we show results obtained from a scene acquired on June-24m, 2003 in the area of Weiterstadt, Hessen. In addition, we present results from a scene close to Rostock, Mecklenburg- Vorpommern acquired on July-27, 2006.

Examples of images, edge images, and derived histograms of ATKIS grassland and croplands objects are shown in Figure 9-Figure 11. In the histogram of grassland of Figure 9 a significant edge direction is not detectable, and the object is accepted by the verification system.

The results presented in Figure 10 indicate that object can be accepted as cropland. Although, the edge image is not as clear as the one in Figure 6, a main direction can still be detected unambiguously.

In contrast to the preceding example, in Figure 11 a successful verification of the cropland object is not possible. The cultivation lines are not separable from the background as can also be seen in the edge image. In the histogram a significant peak can not be detected. The verification system rejects the object – a false negative decision.

For the second scene depicting an area close to Rostock the approach was tested on the whole image compared to the few shown examples of the scene Weiterstadt. An example of a cropland object in this scene is shown in Figure 12. The peak of the main direction is at 12grad. The standard deviation is 3.6grad. In the histogram three peaks are visible. The first peak has the highest occurrence and is the main direction of cultivation. The second peak has an occurrence of less than five and lies below the threshold. This peak is noise in the image caused by disturbances, i.e. in this case the trees inside the field. The third peak is a part of the first one, appearing at approximately 200grad due to the periodicity of the edge direction.

The results of the scene Rostock are investigated using a confusion matrix (Figure 7). The percentage of corresponding acceptance indicates the efficiency of the approach. There will also be undetected errors if objects which have been accepted by the automatic procedure, are rejected by the human operator. The percentage of undetected errors has to be as small as possible.

Automatic / Human Operator	Green	Red
Green	Efficiency	Interactive Final Check
Red	Undetected Errors	Interactive Final Check

Figure 7: Confusion Matrix

In Figure 8 the confusion matrix for the scene Rostock is shown. At this scene 77 cropland objects are checked by a human operator and by our approach. Objects rejected by automatic system need to be checked by the human operator interactively. The threshold t for σ is 5grad, for s a value of 5 is chosen. As shown in Figure 8 the efficiency of our approach is around 55%, the false alarms are 31%. 11 objects (14%) which were wrong in the GIS are detected by the system automatically. Undetected errors are not present.

Automatic / Human Operator	Green	Red
Green	55%	31%
Red	0%	14%

Figure 8: Confusion Matrix of the scene Rostock

3.5 Discussion

The examples show the potential of the approach. In general the presented approach is rather robust, because given all the edge pixels we are only interested in two single value, namely the

Trias-Sanz, R., 2006: Texture Orientation and Period Estimation for Discriminating Between Forests, Orchards, Vineyards, and Tilled Filled. In: *IEEE Transactions on Geoscience and Remote Sensing*, vol. 44, no. 10, Oct. 2006, pp. 2755

Warner, T.A. and Steinmaus, K., 2005: Spatial Classification of Orchards and Vineyards with High Spatail Resolution Panchromatic Imagery. In *Photogramm. Eng. & Remote Sensing*, vol. 71, no.2, Feb. 2005, pp. 179- 187

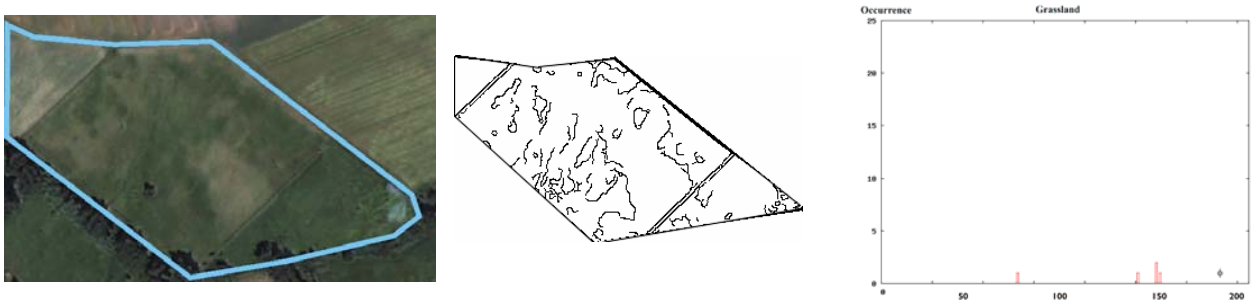

Figure 9: Image space, edge image and histogram of a grassland example (from left to right)

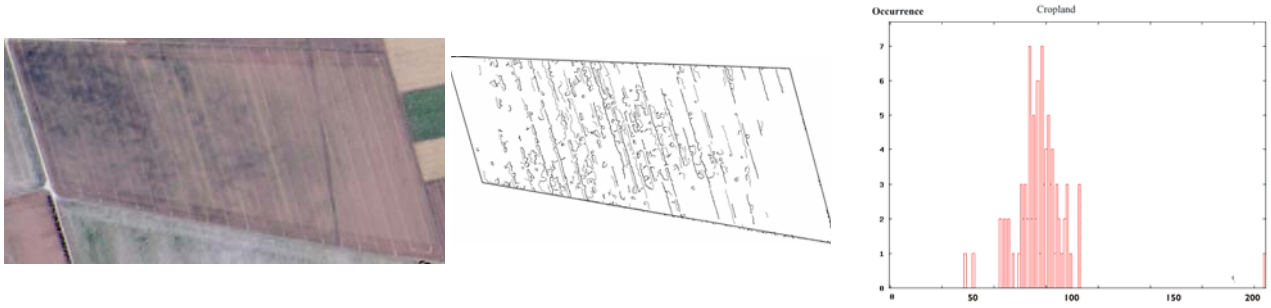

Figure 10: Image space, edge image and histogram of a cropland example (from left to right)

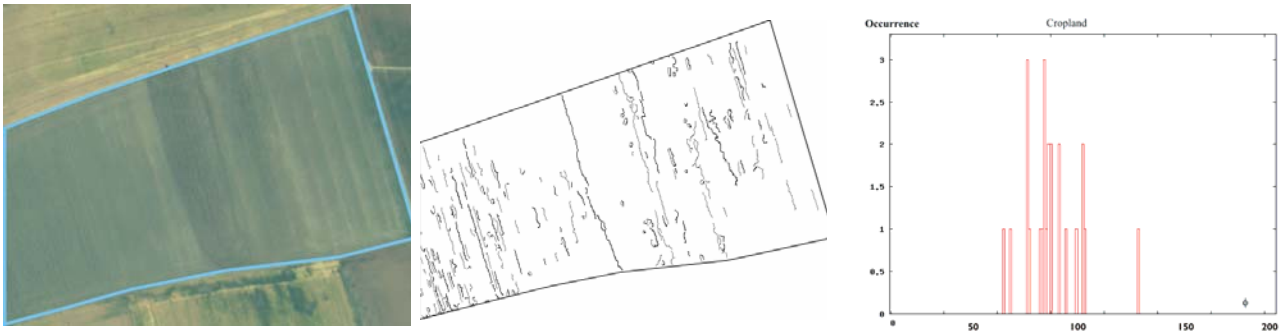

Figure 11: Image space, edge image and histogram of a cropland example (from left to right)

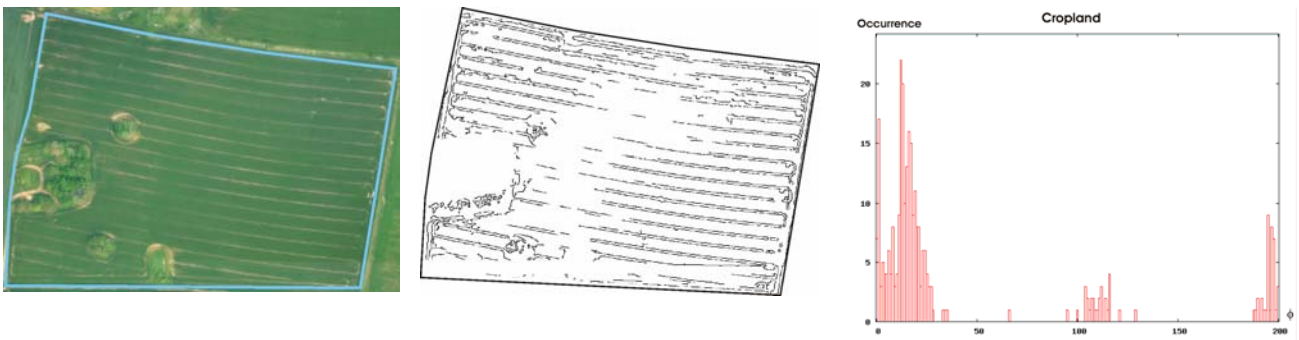

Figure 12: Image space, edge image and histogram of a cropland example (from left to right)